

# Digital Image Correlation Method in Monitoring Deformation During Geogrid Testing

DOI: 10.5604/01.3001.0012.9992

Cracow University of Technology,  
Faculty of Civil Engineering,  
ul. Warszawska 24, 31-155 Kraków, Poland,  
\* e-mail: jgorszcz@pk.edu.pl  
\*\* e-mail: kmalicki@pk.edu.pl

## Abstract

*This article presents the results of tests on geogrids conducted using the Digital Image Correlation (DIC) method and those of numerical simulations of laboratory tests on the geogrid using the wide-width strip method. DIC allowed for the non-contact determination of displacements and strains for the entire surface of the samples of geosynthetics tested. The results of the laboratory tests and numerical simulations have been compared. The results of the tests and analyses indicate that the DIC method is an effective tool for evaluating the parameters of geogrids used in GRS systems and in pavement structures. In addition to the standard deformation image for the averaged base, analysis of deformations in any direction and at any point on the surface of the geogrid is possible. The measurement method applied also opens possibilities for validation of numerical models of geogrids made using the finite element method (FEM).*

**Key words:** geogrid, geosynthetic, digital image correlation, tension tests, finite element method, image analysis.

## ■ Introduction

Geosynthetic reinforced structures are widely used in the construction of transport infrastructure. Many field studies are being conducted along with the development of physical and numerical models aimed at simulating the impact of different factors on the functioning of geosynthetic reinforced structures.

The subject matter of geosynthetic reinforced soil (GRS) systems, particularly in the area of bridge abutments, was widely discussed by Wu et al. [1], Adams et al. [2] and Nicks et al. [3]. The soil in a GRS system is reinforced in layers by using polymer geosynthetics (e.g. geogrids or geotextiles). It was noted that the current design methods are insufficient, as the strains measured are in fact significantly smaller than those determined in design methods [1]. Numerical analyses carried out using the finite element method (FEM) showed the influence of the stiffness of the geosynthetic on the degree of subsidence on the lower surface of the soil layer investigated. It was emphasised that both the tensile strength of the geosynthetic and its stiffness should be selected in such a way as to transfer the occurring load while maintaining an appropriate safety margin. Chen et al. [4] demonstrated that in laboratory tests geosynthetics characterised by a greater stiffness ensure a better functioning of the GRS system than those with lower stiffness.

A similar phenomenon is observed in flexible road pavement structures.

The structure of such a road pavement consists of interconnected layers of asphalt mixtures in the upper section. Between asphalt layers, geosynthetic interlayers are often used. The state of bonding between the layers plays a significant role in the durability of the whole structure. In the absence of an adequate bond, interlayer bond weakening and acceleration of road pavement structure degradation occur [5-7].

Thus in order to achieve the correct modelling, design and construction of geosynthetic reinforced structures, it is necessary to define in a precise way the strains and stresses occurring in geosynthetics subject to bearing loads, which includes their stiffness. The continuous development of these products indicates the need for the simultaneous development and introduction of new test methods allowing a full and strict assessment of their mechanical parameters.

According to the standard procedure for testing geosynthetics by the method of wide-width strips [8], measurement of the deformation of the material tested is carried out in one direction under analysis, the so-called base, without providing information about strains across the whole surface of the geosynthetic specimen tested.

This article presents the results of tests of geogrids carried out using the two-dimensional Digital Image Correlation (DIC) method. This method is used to monitor the deformation of the geogrid

during testing, instead of using the more conventional method of measurement.

Moreover the results obtained through contact extensometers and the DIC method were compared. A system based on the DIC method allows for a contactless determination of displacements and strains of specimens in static and fatigue tests, based on an optical analysis of the material deformation [e.g. 9, 10]. The main advantage of the system is the possibility to analyse the deformation of all points on the surface of the specimen monitored during the test. A DIC system can be implemented on a properly prepared laboratory workstation to perform mechanical and thermo-mechanical tests on specimens of different materials and with various geometry [e.g. 11-14]. Youngguk et al. [9], Birgisson et al. [15] and Safavizadeh et al. [16] claim that the DIC method is an effective tool in strength tests of specimens of bitumen-aggregate mixtures. According to Oats et al. [17], it can be effectively used to evaluate the displacement and damage to existing bridge objects.

The present article also provides a numerical model of testing geogrids using the method of wide-width strips, employed for determining the strength of geogrids used e.g. in GRS systems, or for the reinforcement of pavement structures. The model included two geogrids of varying stiffness. The results of numerical simulations were compared with those of the laboratory tests, indicating the areas in which the DIC method provides

a better description of the functioning of the geogrids in a tension test compared to the traditional contact extensometers.

## Laboratory test methods

### Method of digital image correlation

The two-dimensional DIC system allows to determine deformations of a geosynthetic tested in any direction and at any point without the use of extensometers. It also allows to solve the issues of principal strains and principal directions for the surface analysed. This system can be successfully applied for the determination of Young's modulus and Poisson's ratio [18]. The history of the method, basic concepts, theory and different applications have been described by Sutton et al. [19].

The main elements of the system are cameras, a controller and a computer with the appropriate software. A functional diagram of the laboratory test based on the DIC method is shown in *Figure 1*.

The system's digital camera, which parses the area, finds characteristic points on the surface of the geosynthetic tested that become reference points for a virtual grid/discretisation of the surface analysed. Based on the changes in the distance between points registered, and on the numerical evaluation, a map of displacements and strains is created for the entire surface of the test material seen by the camera. The results of the measurements can be presented graphically in the form of graduated colour maps.

In the analyses of changes in the position of the points on the surface of the specimen tested, two models are used: the first one based on the normalised cross-correlation (NCC), and the second on the selection of the least-squares matching (LSM) [10, 19, 20]. In the NCC method, for each position one calculates the cross-correlation coefficient  $\rho$  between the reference (undeformed state) and current location of the points (deformed state). The nearest location at the pixel level is selected by choosing the minimum value of the mutual normalised cross-correlation coefficient. The normalised correlation function is estimated in the area investigated, while its maximum indicates the best match. The  $\rho$  coefficient is calculated with a discrete function of displacement  $(\Delta x, \Delta y)$  in accordance with the *Equation (1)* [10, 19], where  $\hat{f}$  and  $\hat{g}$

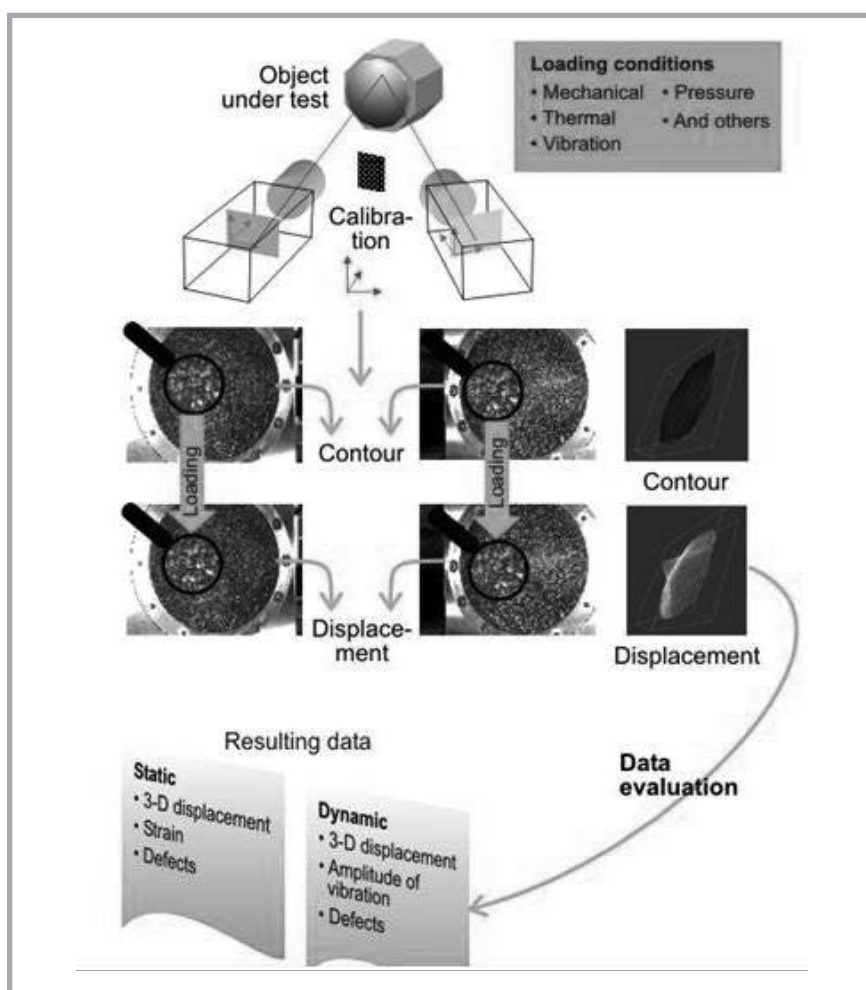


*Figure 1. Functional diagram of a DIC system [18].*

are the mean values of the grey levels of compared windows.

The NCC method algorithm is faster, however it only considers the shifts of sets of points on the vertical and horizontal axis, without taking into account their rotations. The LSM method uses more complex models and equations, allowing for considering both the translation and rotation of a set of points. The best match is defined by minimising the difference in gray levels between two consecutive steps (images) of the analysis using the method of least squares. An adjustment of parameters taking into account shifts and rotations is determined in accordance with *Equation 2*, in which  $(a_1, a_2, b_1, b_2)$  are variable parameters of shape,  $(a_3, b_3)$  – parameters of shift,

$e(x_1, y_1)$  – the residual function for point  $(x_1, y_1)$  in the reference image of the area (undeformed), and  $(r_0, r_1)$  are, respectively, the parameters of brightness change and image contrast during the test [10, 19]:

$$f(x_1, y_1) + e(x_1, y_1) = r_0 + r_1 \cdot g(x_2(u, v), y_2(u, v)) = \hat{g}(r_0, r_1, a_1, a_2, a_3, b_1, b_2, b_3) \quad (2)$$

Function  $\hat{g}(r_0, r_1, a_1, a_2, a_3, b_1, b_2, b_3)$  is linearised and solved using the Gauss – Markov least squares estimation method.

### Tension testing of geosynthetics using the method of wide-width strips

Tensile tests were conducted based on the standard EN ISO 10319:2015 [8]. Ac-

$$\rho = \frac{\sum_x \sum_y (f(x, y) - \hat{f}) \times (g(x + \Delta x, y + \Delta y) - \hat{g})}{\left( \sum_x \sum_y (f(x, y) - \hat{f})^2 \times \sum_x \sum_y (g(x + \Delta x, y + \Delta y) - \hat{g})^2 \right)^{\frac{1}{2}}} \quad (1)$$

*Equation 1.*

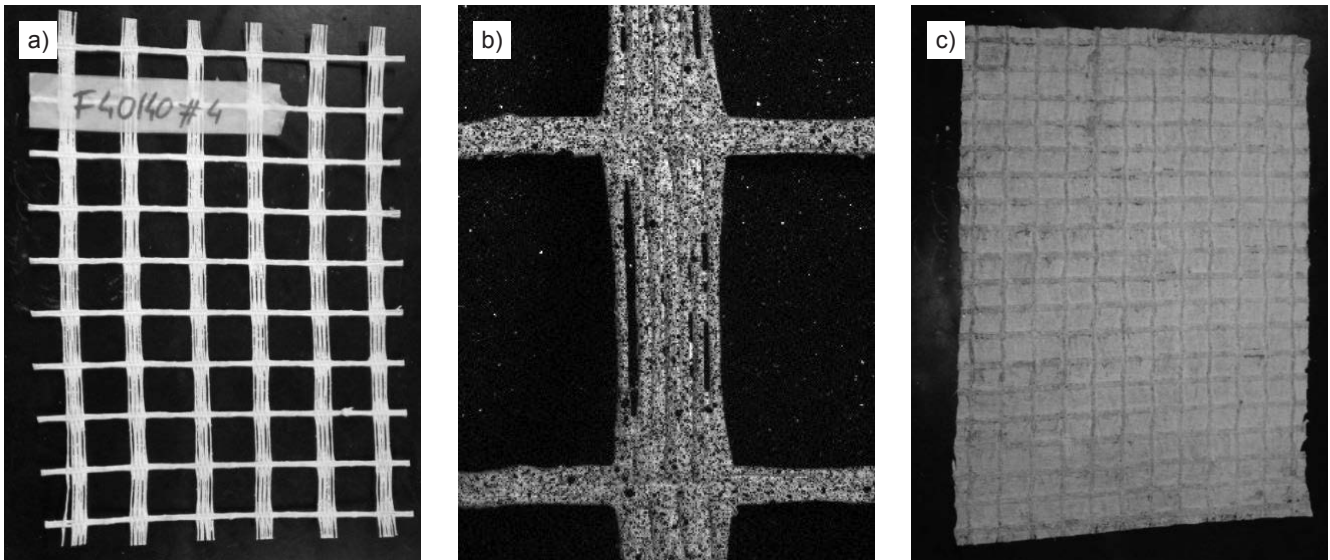


**Figure 2.** Specimens of geosynthetics prepared for testing: a) polyester geogrid, b) enlarged image of polyester ribs, c) glass geogrid.

According to the procedure of the standard, determination of the specimen deformation is made on the basis of the registration of changes in the length of the 60 mm measurement base situated in the central part of the specimen in a direction parallel to that of the tensile force applied. The standard allows for the measurement of deformations using mechanical, optical and infrared equipment, or any other with an electrical output. Samples 200 mm wide and 100 mm long between

the jaws were prepared for the tests. The number of specimens was 5 for each direction tested.

### Laboratory specimens and test workstation

#### Geosynthetics used in the research

The research used specimens prepared from polyester geogrid and glass geogrid. Polymer geosynthetics are intended for use in the construction of transport

infrastructure, among others, for GRS systems, strengthening weak ground, reinforcing embankments and stabilising landslides [e.g. 21-26]. The glass geogrid intended for reinforcing asphalt layers [5, 6] is made of glass fibres and coated with a bituminous layer, with sand sprinkled on one side and a protective polyester foil preventing the material from sticking together during storage [27].

#### Specimen preparation

Twenty specimens of geosynthetics with dimensions of  $20 \times 30$  cm each were prepared for testing. The surface of the specimens to be measured using DIC required special preparation. To begin with, the specimens were coated with a layer of white paint. Next black paint was sprayed over the surface thus prepared, creating a pattern of small, black points on a white background. The specimens prepared for testing are shown in **Figure 2**. **Figure 3** depicts digital grid/discretisation of the DIC method for the specimens.

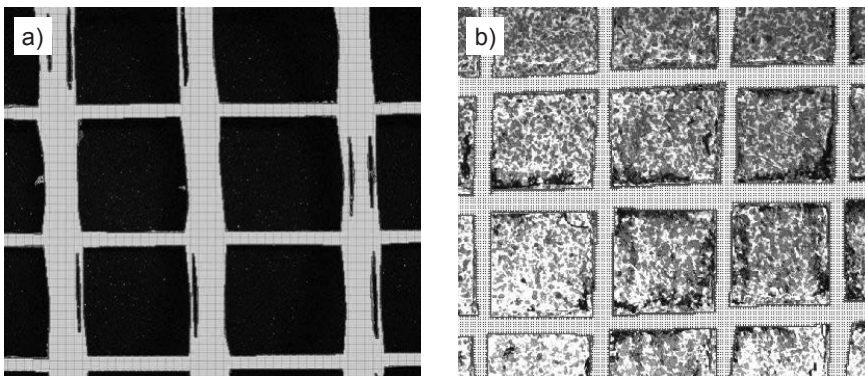


**Figure 3.** Grid of DIC method: a) specimen of polyester geogrid, b) specimen of glass geogrid.

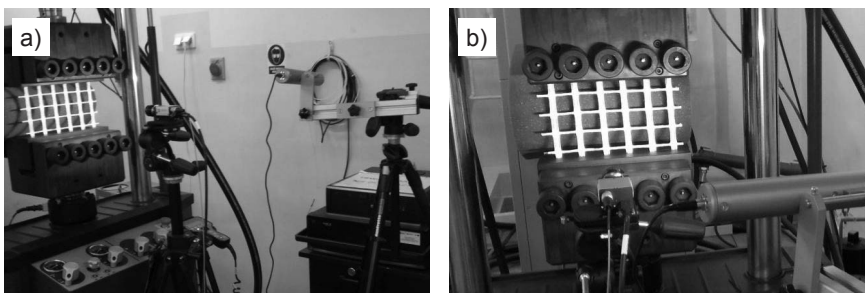


**Figure 4.** Laboratory stand for geosynthetic testing using the DIC method: a) side view, b) front view.

#### Testing workstation and test parameters

The testing of geosynthetics was conducted in a laboratory test setup whose key elements are as follows [23]: a servo-hydraulic testing machine, a controller, + a computer controlling the DIC system, a DIC system digital camera, and appropriate linear lighting.

The research was conducted at a temperature of  $+ 20$  °C, while the speed of the deformation was equal to 20 mm/min for polyester geogrid and 2 mm/min for

glass geogrid [8]. The rate of deformation during the test depends on the expected maximum value of strain when the sample is damaged. The test setup is shown in *Figure 4*.

### Finite element model of the tensile tests of geosynthetics

The following elements in ANSYS code were used from ANSYS software in FE modelling of the tensile tests of geosynthetics using the wide-width strips method: 20-node, solid element SOLID186, 8-node SURF154, and contact surfaces between the body were modelled with 8-node elements of TARGE170 and CONTA174. The geogrid was modelled by elements with only the tensile stiffness: the 4-node anisotropic 2-dimensional element SHELL41 and the 2-node anisotropic element LINK180 [28]. The quality of the mesh was tested. A sufficient number of elements were selected that gave the correct solution accuracy. The final number of elements for the model with a polyester geogrid was equal to 2438. For the FEM model with a glass geogrid, it was equal to 1356 elements. The final mesh of the model is shown in *Figure 5*.

A material model of the geosynthetics was formulated using Hooke's Law. The elastic modulus determined in the geogrid laboratory tensile tests was  $E = 7600$  MPa for the polyester geogrid and  $E=44500$  MPa for the glass geogrid [29]. Poisson's ratio was  $\nu = 0.20$  for the glass geogrid and  $\nu = 0.35$  for the polyester geogrid [29]. The choice of Young's modulus is crucial in the accuracy of FEM results.

The models were analysed as non-linear. Solutions were computed by the iterative Newton-Raphson procedure.

### Results of laboratory tests and fem analysis

*Tables 1* and *2* provide a comparison of the values of vertical strain according to Standard [8], designated using two measurement techniques and FEM analysis for different levels of load. The results which were obtained showed no significant differences, pointing to the correct operation of the DIC system and its additional capabilities. Post processing included smoothing the results obtained us-

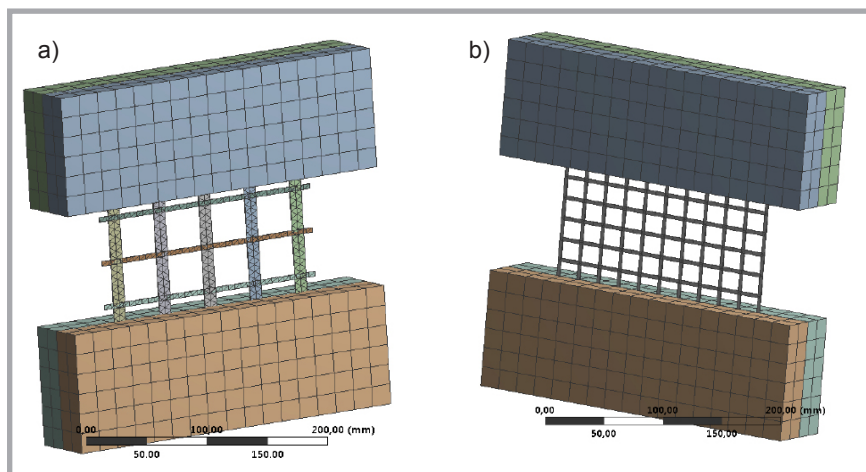


*Figure 5.* Mesh of the FEM model of the tensile tests: a) specimen of polyester geogrid (SHELL41), b) specimen of glass geogrid (LINK180).

*Table 1.* Average values of deformations of 5 specimens - polyester geogrid.

Load, kN	Vertical strain $\times 10^4$ , mm/mm		
	Extensometer	DIC (average for a 60 mm base)	FEM
2.64	300	336	287
6.27	600	656	681
10.83	900	967	1169

*Table 2.* Average values of deformations of 5 specimens - glass geogrid.

Load, kN	Vertical strain $\times 10^4$ , mm/mm		
	Extensometer	DIC (average for a 60 mm base)	FEM
18.49	200	211	189
22.10	250	274	228
16.89	300	325	—

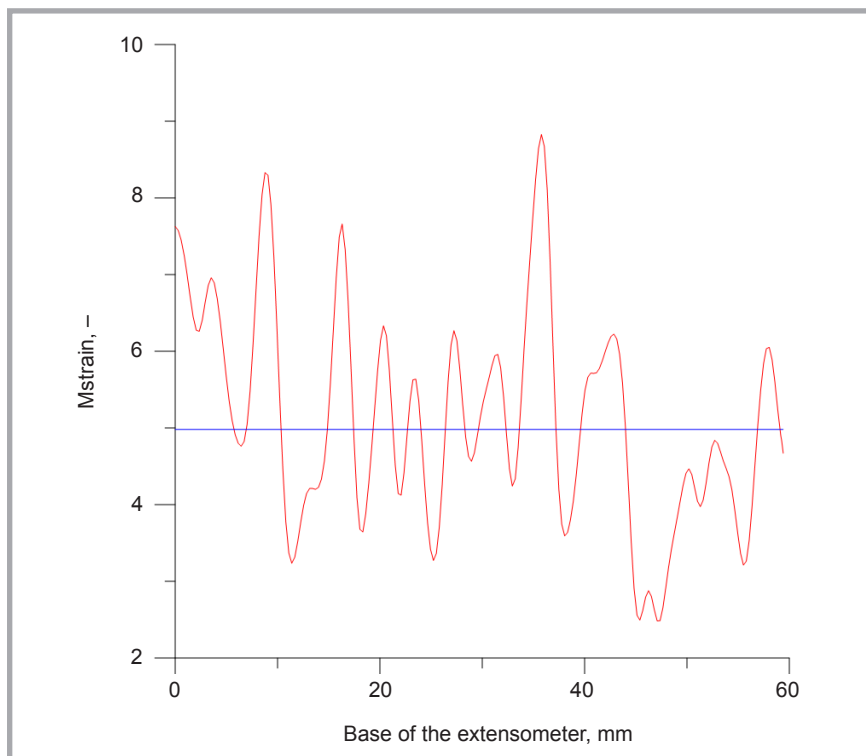


*Figure 6.* Variation of the vertical strain in the base of the extensometer (red) vs the strain of the geosynthetic specimen (glass geogrid), determined using an extensometer (blue) with load 4.5 kN.

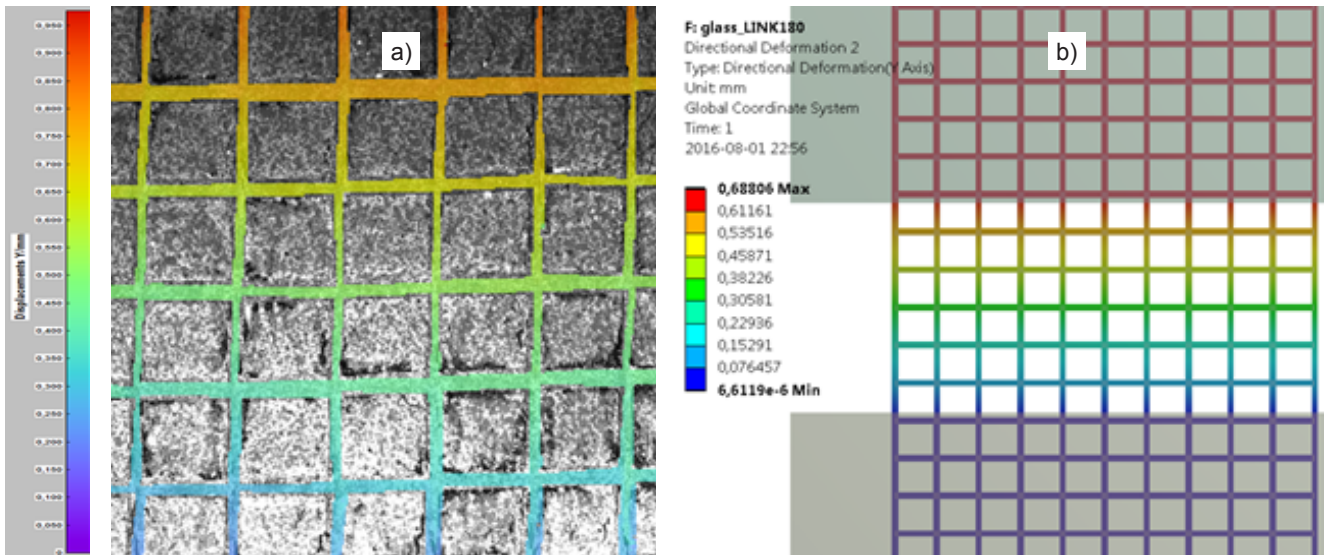


**Figure 7.** Distribution of vertical displacements [mm] on the surface of a specimen of the glass geogrid, load 5.0 kN: a) results obtained using DIC method, b) results obtained using FEM.

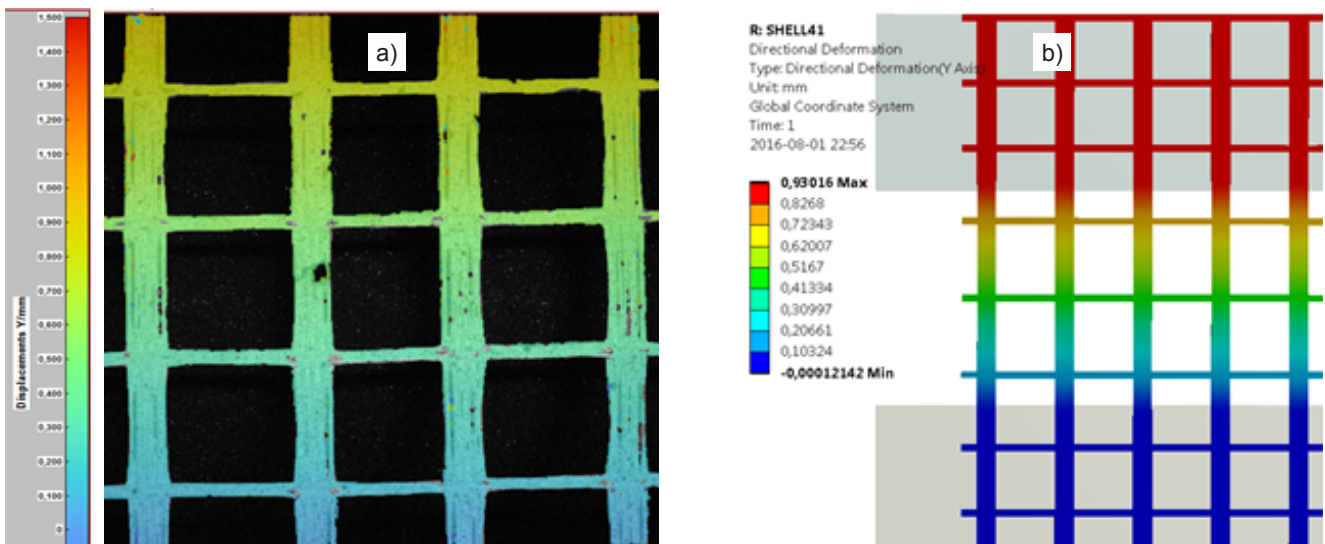


**Figure 8.** Distribution of vertical displacements [mm] on the surface of a specimen of the polyester geogrid, load 2.5 kN: a) results obtained using DIC method, b) results obtained using FEM.

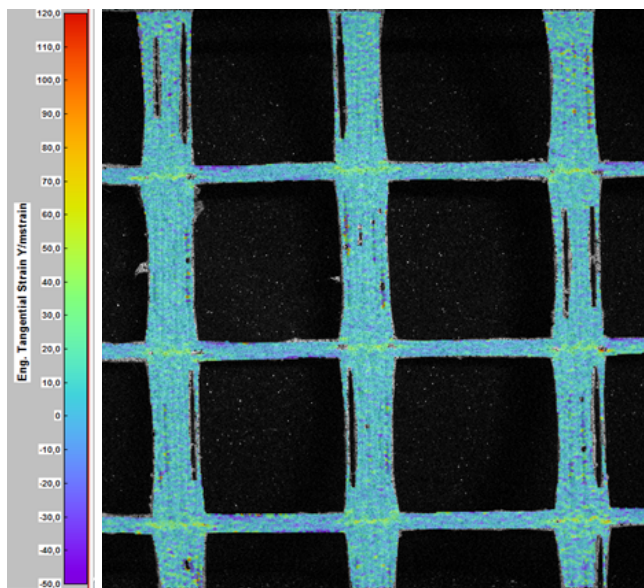


**Figure 9.** Distribution of vertical mstrain on the surface of a specimen of the polyester geogrid, load 1.5 kN; results were obtained using DIC method.

ing an adaptive spline polynomial algorithm [18], and the maximum uncertainty of the true principal strains was equal to 0.5%. **Figure 6** (see page 87) shows a graph of the vertical strain changes of a geosynthetic specimen, designated using the DIC system within the traditional measurement base of the extensometer.

Selected results of laboratory tests, and those obtained using FEM in the form of colour maps are shown in **Figures 7-10**.

## Conclusions

The results of research and analyses of the geosynthetics conducted allowed to formulate the following conclusions:

- The two-dimensional Digital Image Correlation (DIC) method implemented at a properly prepared laboratory workstation enabled an effective measurement of the deformation of the geosynthetics in a tension test using the wide-width strips method.
- The method employed allows one to specify the comprehensive surface character of the geosynthetic tested, yielding the possibility to designate exhausted places, as well as those outside of the base, which can affect the strength and displacements of geosynthetics in geosynthetic reinforced structures (**Figures 9 and 10**).
- The ability to designate displacements and strains for the entire surface of geosynthetic specimens along with a solution of the issues of principal strains and principal directions is a great advantage of the method, as it cannot be obtained using traditional methods of measurement – extensometers (**Figures 7, 8 & 10**).
- The measuring method applied also opens possibilities for validating models of geosynthetics produced using the finite element method (FEM).
- The DIC method allows to fully take into account and illustrate the specific deformation of geogrids of varying stiffness in strength tests as heterogeneous and anisotropic structures, which can be used, for example, in GRS systems or road pavement structures (**Figure 9**).
- The numerical algorithm applied allows to eliminate the movement of the specimen as a rigid body during the test. This allows, for example, to limit the impact of the problem associated with the possibility of the geosynthetic specimens slipping out from the jaws of the test equipment.
- This article presents the results of the first tests, while a full and optimal use of the DIC method in strength tests of geosynthetics requires further implementation works.
- In the work to follow, research will include three- and four-axis geosynthetics and geocomposites. It is believed that the DIC method will allow analysis of the impact of the nodes on the operation of the entire geosynthetic and will create a possibility for analysis of the strains of particular components in composite systems.

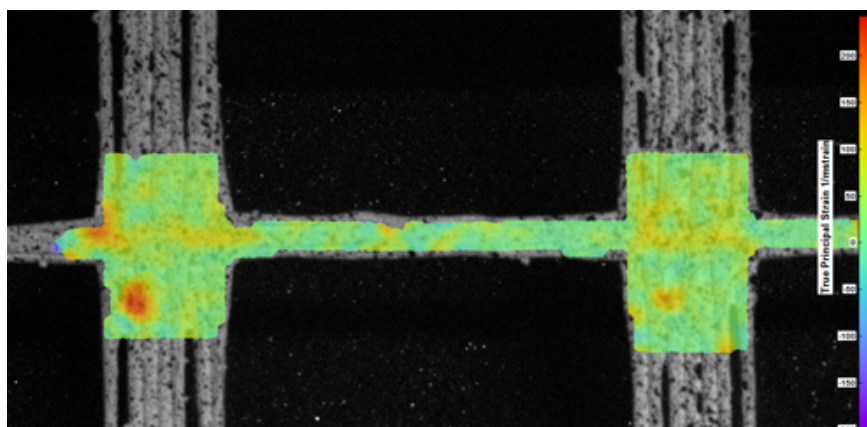


**Figure 10.** Distribution of maximum principal strain on the surface of the nodes of a specimen of the polyester geogrid, load 2.5 kN.

## References

1. Wu JTH, Lee KZZ, Helwany SB, Ketchart K. *Design and Construction Guidelines for Geosynthetic Reinforced Soil Bridge Abutments with a Flexible Facing*. NCHRP REPORT 556. University of Colorado at Denver, Denver, CO. Transportation Research Board of the National Academies, Washington, D.C., 2006.
2. Adams M, Ketchart K, Ruckman A, Dimillio AF, Wu J, Satyanarayana R. *Reinforced Soil for Bridge Support Applications on Low-Volume Roads*. Transportation Research Record: Journal of the Transportation Research Board of the National Academies, Washington, D.C., no. 1652, 150-160, 1999.
3. Nicks J E, Adams M, Wu J. A new approach to the design of closely spaced geosynthetic reinforced soil for load bearing applications. Transportation Research Board of the National Academies, *92th Annual Meeting*, Washington, D.C., 2013.
4. Chen Q, Abu-Farsakh M Y, Sharma R, Zhang X. Laboratory Investigation of the Behavior of Foundations on Geosynthetic Reinforced Clayey Soil. Transportation Research Record: Journal of the Transportation Research Board, Transportation Research Board of the National Academies, Washington, D.C., no. 2004, 28-38, 2007.
5. Górszczyk J, Gaca S. The influence of the carbo-glass geogrid-reinforcement on the fatigue life of the asphalt pavement structure, *Archives of Civil Engineering* 2012; 58, 1: 97-113.
6. Szydło A, Malicki K. Analysis of the correlation between the static and fatigue test results of the interlayer bondings of asphalt layers. *Archives of Civil Engineering* 2016; 62, 1: 83-98.
7. Judycki J, Jaskuła P, Pszczoła M, Dołycki B, Stienss M. New polish catalogue of typical flexible and semi-rigid pavements. *MATEC Web of Conferences* 2017; 122, 04002.
8. EN ISO 10319:2015 Geosynthetics, Wide-width tensile test (ISO 10319:2015). European Committee for Standardization.
9. Youngguk S, Kim Y R, Witczak M W, Bonaquist R. Application of Digital Image Correlation Method to Mechanical Testing of Asphalt-Aggregate Mixtures. Transportation Research Record: Journal of the Transportation Research Board of the National Academies, Washington, D.C., no. 1789, 162-172, 2002.
10. Romeo E. Two-dimensional digital image correlation for asphalt mixture characterisation: interest and limitations. *Road Materials and Pavement Design* 2013; 14, 4, 747-763.
11. Romeo E, Montepara A. Characterization of reinforced asphalt pavement cracking behavior using flexural analysis. *SIIV – 5th International Congress – Sustainability of Road Infrastructures, Procedia – Social and Behavioral Sciences* 2012, 53, 356-365.
12. Szymczak T, Grzywna P, Kowalewski Z L. Modern methods for determination of mechanical properties of engineering materials. *Transport samochodowy* 2013, 1: 79-104.
13. Siebert T, Crompton M J. Application of High Speed Digital Image Correlation for Vibration Mode Shape Analysis. *Proceedings of the SEM Annual Conference*, Indianapolis, Indiana USA ©2010 Society for Experimental Mechanics Inc, June 7-10, 2010.
14. Górszczyk J, Malicki K. Laboratory tests of the selected mechanical properties of the soil stabilized with a road binder. *17th International Multidisciplinary Scientific GeoConference SGEM 2017*, Conference Proceedings Vol. 17, Science and Technologies in Geology, Exploration and Mining, Issue 12, Albena, Bulgaria, 491-498, 2017.
15. Birgisson B, Montepara A, Napier J, Romeo E, Roncella R, Tebaldi G. Micromechanical Analyses for Measurement and Prediction of Hot-Mix Asphalt Fracture Energy. Transportation Research Energy.

- cord: Journal of the Transportation Research Board, Transportation Research Board of the National Academies, Washington, D.C., no. 1970, 186-195, 2006.
16. Safavizadeh SA, Wargo A, Guddati M, Kim YR. Investigation of Reflective Cracking Mechanisms in Grid-Reinforced Asphalt Specimens Using Four-Point Bending Notched Beam Fatigue Tests and Digital Image Correlation. *Transportation Research Record: Journal of the Transportation Research Board, Transportation Research Board of the National Academies, Washington, D.C., no. 2507, 29-38, 2015.*
  17. Oats RC, Harris DK, Ahlborn TM, de Melo e Silva HA. "Evaluation of the Digital Image Correlation Method As a Structural Damage Assessment and Management Tool". *Transportation Research Board of the National Academies, 92th Annual Meeting, Washington, D.C., 2013.*
  18. Digital Image Correlation for Deformation Measurement. Dantec Dynamics. <http://www.dantecdynamics.com>.
  19. Sutton MA, Orteu J, Schreier HW. *Image Correlation for Shape, Motion and Deformation Measurements. Springer Science+Business Media, LLC, New York, 2009.*
  20. Huang YH, Liu L, Sham FC, Chan YS, Ng S P. Optical strain gauge vs. traditional strain gauges for concrete elasticity modulus determination. *Optik – International Journal for Light and Electron Optics* 2010; 121: 18.
  21. Fortrac – Immensely Versatile Solutions for Reinforced Soil, 11/15 B HUESKER Synthetic GmbH, Gescher 2015. <http://www.huesker.com>, <http://www.huesker.pl>.
  22. Fortrac geogrids in geosynthetic reinforced soil systems, (in Polish). Przedsiębiorstwo realizacyjne Inora Sp. z o. o. 2nd edition. <http://www.inora.pl>.
  23. Górszczyk J, Malicki K. Study of the mechanical properties of a hexagonal geogrid using the digital image correlation method. *17th International Multidisciplinary Scientific Conference on Earth & Geosciences SGEM 2017*. Conference Proceedings Vol. 17, Science and Technologies in Geology, Exploration and Mining, Issue 12, Albena, Bulgaria, pp. 809-816, 2017.
  24. Górszczyk J, Malicki K. Three-dimensional finite element analysis of geocell-reinforced granular soil. *18th International Multidisciplinary Scientific GeoConference SGEM 2018*, Conference Proceedings Vol. 18, Science and Technologies in Geology, Exploration and Mining, Issue 1.2, Albena, Bulgaria, 735-742, 2018.
  25. Górszczyk J, Malicki K, Sławińska M. Structural analysis of soil reinforced by geocell system using analytical-empirical method. *18th International Multidisciplinary Scientific GeoConference SGEM 2018*. Conference Proceedings Vol. 18, Science and Technologies in Geology, Exploration and Mining, Issue 1.2, Albena, Bulgaria, 669-676, 2018.
  26. Grygierek M, Kawalec J. Selected laboratory research on geogrid impact on stabilization of unbound aggregate layer. *Procedia Engineering* 2017; 189: 484-491.
  27. Technical Data Sheet S&P Glasphalt G, S&P Clever Reinforcement Company AG, Seewernstr. 127 CH-5423 Seewen, VER07/15\_HUM, <http://www.sp-reinforcement.eu>.
  28. ANSYS Inc. Documentation for ANSYS 10.0. 2005 SAS IP.
  29. Górszczyk J. Influence of the geosynthetic reinforcement on fatigue life of the asphalt pavement. PhD dissertation, Cracow University of Technology, 2010.

Received 25.10.2018 Reviewed 31.01.2019

2019  
IWTO



88th Congress  
VENICE / 9-11 April

PLASTIC  
FREE WORLD  
CONFERENCE & EXPO  
FRANKFURT, 27/28 JUNE 2019

